Adv. Space Res. Vol. 11, No. 11, pp. (11)5–(11)14, 1991
Printed in Great Britain.

0273–1177/91 $0.00 +.50

PEEKING THROUGH THE PICKET FENCE: WHAT ASTROPHYSICAL SURPRISES MAY BE PRESENT IN THE 100–1200 Å REGION?

Jeffrey L. Linsky and Donald G. Luttermoser

Joint Institute for Laboratory, Astrophysics, National Institute of Standards and Technology, University of Colorado, Boulder, CO 80309-0440, U.S.A.

ABSTRACT

In anticipation of more sensitive EUV and FUV spectroscopic instruments, we simulate spectra, including interstellar absorption, of solar-like, RS CVn, and flare stars as folded through the instrument parameters of the EUVE, Lyman/FUSE Phase A, and a desirable next-generation spectrometer. We find that even the relatively insensitive EUVE spectrometer will be able to detect sufficient spectral lines from many active binary and dMe stars to determine their coronal emission measure distributions. The Lyman/FUSE or next-generation spectrometers are needed to study solar-type stars or flaring stars with high time resolution. The high throughput and effective area of a next-generation spectrometer is needed for Doppler imaging studies, stellar wind and downflow measurements, and high time and spectral resolution of stellar flares.

INTRODUCTION

This meeting on "EUV and FUV Astrophysics of Stars" occurs at the threshold of a very rapid increase in the data anticipated in these new spectral regions.

- Until now spectrometers on Voyager and EXOSAT have provided only limited glimpses of a few hot white dwarfs and other hot stars in the EUV (100–912 Å). We look forward to spectra of many stars of diverse types from the HUT instrument on Astro-1, ORFEUS on ASTROSPAS, the EUVE spectrometer, and the EUV channel on Lyman/FUSE.

- Until now sounding rockets have provided a few low-resolution images of the EUV sky. We look forward to the feast of data expected from the the Wide Field Camera on ROSAT and the all-sky and deep surveys with EUVE.

- Until now, *Copernicus* has obtained FUV (912–1200 Å) spectra of only a limited number of stars located within 1 kpc, which have provided valuable information on the properties of interstellar gas on the lines of sight towards these stars. We look forward to high-resolution spectra of nearly all types of stars in the Galaxy and the brighter sources in many other galaxies, which will be provided by Lyman/FUSE.

We introduce the session by summarizing the important features in solar FUV and EUV spectra and then present simulated spectra of solar-type and active late-type stars that should be detected by spectrometers planned for EUVE, Lyman/FUSE, and by a hypothetical next-generation spectrometer with enhanced throughput and spectral resolution. These simulations will allow us to extrapolate our present understanding of stellar chromospheres, coronae and flares into two nearly unexplored spectral regions. Missions being planned to observe celestial sources in these new spectral regions should confirm or refute our present paradigms, which are based on solar analogy, and more importantly should discover new phenomena and new types of stars. We suggest how one might proceed to make such discoveries.

[1]Staff Member, Quantum Physics Division, National Institute of Standards and Technology

SPECTRA OF SOLAR-TYPE STARS

The solar FUV spectrum provides a convenient first approximation to spectra of late-type dwarf stars, spectroscopic binaries, and perhaps a broader range of stellar types. Table 1 lists the brightest emission lines for a solar active region /1/ in order of decreasing intensity with lines grouped according to degree of ionization. The line intensities in active regions are typically ten times larger than for quiet regions, and the emission lines are much brighter than the underlying continuum for both active and quiet regions. While $L\alpha$ dominates the solar spectrum in this region, $L\beta$ is comparable in flux to the lines of SiIII and CIII, formed at roughly 60,000 K, and the lines of OVI, formed at 300,000 K. Higher members of the Lyman series are much fainter. In stellar spectra interstellar absorption will remove most or all of the flux in $L\alpha$, so that the SiIII, CIII, and OVI lines will likely dominate the observed spectra. The solar active region spectrum should be a good approximation to the spectra of dMe and RS CVn stars as these stars typically have surface fluxes 10-30 times that of the quiet Sun in the CIV lines, which are formed at 100,000 K /2,3/.

Table 1. Strongest Lines in Solar Active Regions

FUV (912–1250 Å)						EUV (148–350 Å)				
λ (Å)	HI	I-II	III-IV	V-VI	Intensity	λ(Å)	Low	Medium	High	Flux
1216	$L\alpha$				61,800	304	HeII			11,490
1206			SiIII		630	284			FeXV	2960
977			CIII		410	335			FeXVI	2340
1025	$L\beta$				314	195		FeXII		880
1176			CIII		288	256	HeII			820
1032				OVI	230	180	FeXI			700
1037				OVI	151	211			FeXIV	680
972	$L\gamma$				94	188	FeXI			650
1238				NV	83	193		FeXII		630
1085		NII			77	171	FeIX			580
1242				NV	57	274			FeXIV	550
991			NIII		52	174	FeX			520
949	$L\delta$				46	334	CaVI			470
1200		NI			46	264			FeXIV	410
1194		SiII			30	177	FeX			360
937	$L\epsilon$				25	347	SiX			350
1128			SiIV		25	252			FeXIV	270
923			NIV		25	220			FeXIV	210
930	$L\zeta$				20					
1122			SiIV		19					
1190		SiII			18					
1157		CI			13					
933				SVI	12					
1010		CII			10					
944				SVI	10					

Intensity units: 10^{12} ph cm^{-2} s^{-1} ster^{-1}.
Flux units: 10^{6} ph cm^{-2} s^{-1}.

Emission lines formed at higher temperatures dominate the solar spectrum below the 912 Å photoionization edge of hydrogen, but this same opacity source in the interstellar medium and HeI absorption below 504 Å should completely absorb the spectra of nearly all stars in the 350–912 Å range (see below). Table 1 lists the solar emission line fluxes in the 148–350 Å region observed by OSO-5 /4/ for the very active Sun (sunspot number 194). We note that the bright lines of FeIX-XI are formed at logT = 5.9–6.1 K and the lines of FeXIV-XVI are formed at logT = 6.3–6.5 K. The 90–140 Å region, which is the shortest wavelength region that will be observed by the EUVE and Lyman/FUSE spectrometers, is dominated by $2s^2 2p^k - 2s^1 2p^{k+1}$ transitions of FeXVIII–XXIII, which are formed over the temperature range logT = 6.9–7.5 K /5/. The 100–350 Å region also contains a rich spectrum of line ratios (e.g. for FeXII–XV) that are sensitive to densities in the range $10^8 - 10^{12}$ cm^{-3} /6,7/.

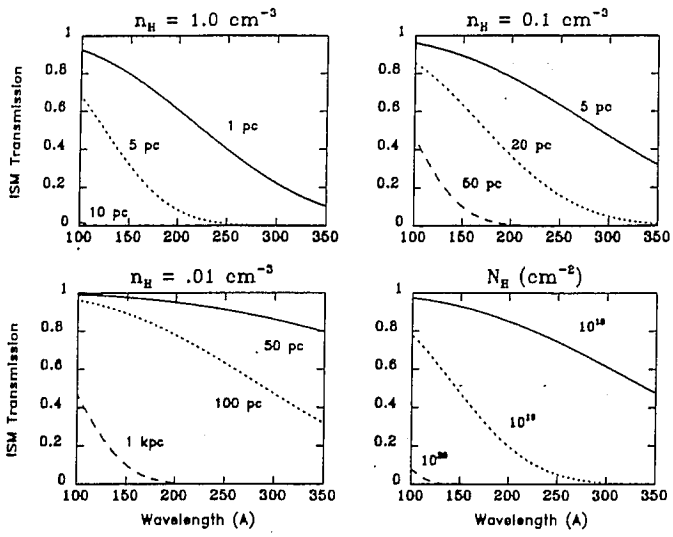

Figure 1: Transmission of the interstellar medium as a function of wavelength and distance for different values of the neutral hydrogen density. The lower right plot shows the transmission for different values of the hydrogen column density.

THE LOCAL INTERSTELLAR MEDIUM

In the current picture of the local interstellar medium (LISM) /8,9/ the Sun is located in an irregularly-shaped region of warm and mostly neutral gas with $n_H \leq 0.1$ cm^{-3}. This region may only extend ≈ 10 pc towards the galactic center, where it comes up against a high-density cloud. The LISM appears to contain a number of velocity components and its structure perpendicular to the galactic plane is not well known at this time. As shown in Figure 1, the EUV horizon depends critically on the wavelength and column density of neutral hydrogen towards a star. If the LISM were a uniform $n_H = 0.1$ cm^{-3}, then we might expect to observe stars beyond 50 pc only for $\lambda \leq 150$ Å. The observed low column densities towards stars in the third quadrant (galactic longitudes $200° - 270°$) to at least 200 pc indicates that hot, low density gas ($n_H \approx 0.01$ cm^{-3}) must extend beyond the local cloud in this direction. In our simulated spectra we assume that $n_H = 0.1$ cm^{-3} along the line of sight towards each star, but this is only a rough estimate.

SIMULATED STELLAR SPECTRA

We compute simulated spectra folded through the response functions of three instruments – the EUVE spectrometer /10/, the proposed Lyman/FUSE high-throughput EUV channel /10/, and a hypothetical high-resolution spectrometer (EUVHRS). The spectral resolutions and effective areas are shown in Figure 2. We also compute simulated FUV spectra for the prime spectrometer on Lyman/FUSE, assuming a resolution $\lambda/\Delta\lambda = 30,000$ and effective area of 50 cm^2 for 900 Å $\leq \lambda \leq$ 1025 Å and 100 cm^2 for 1025 Å $\leq \lambda \leq$ 1250 Å.

We first compute average quiet Sun spectra (Fig. 3) folded through the response functions of the three spectrometers (Fig 2). For each spectrometer we compute the intrinsic spectrum (ignoring the very bright HeII 304 Å line) and the spectrum including only interstellar hydrogen absorption with the indicated neutral hydrogen column density computed from $n_H = 0.1$ cm^{-3} and the indicated distance. The distances to the sources are obtained by requiring that the total count rate in the 100–350 Å band (excluding the HeII 304 Å line) exceed 1000 counts in 50,000 seconds. Our detection criterion of 1000 counts was set to permit the detection of some 30 lines, which should be sufficient to derive the emission measure distribution with temperature in the stellar corona. By this criterion the detection horizon for a solar-type star is only 2.4 pc for the EUVE spectrometer, but 18 pc for the EUVHRS. Most of the emission lines in Table 1 are detected in these simulations, except that interstellar absorption precludes detection of the FeXVI 335 Å line for a star like the quiet Sun located at 18 pc. Simulated spectra of the quiet and active Sun (Fig. 4) indicate that the detection horizons using the Lyman/FUSE Prime spectrometer are 33 and 100 pc, respectively.

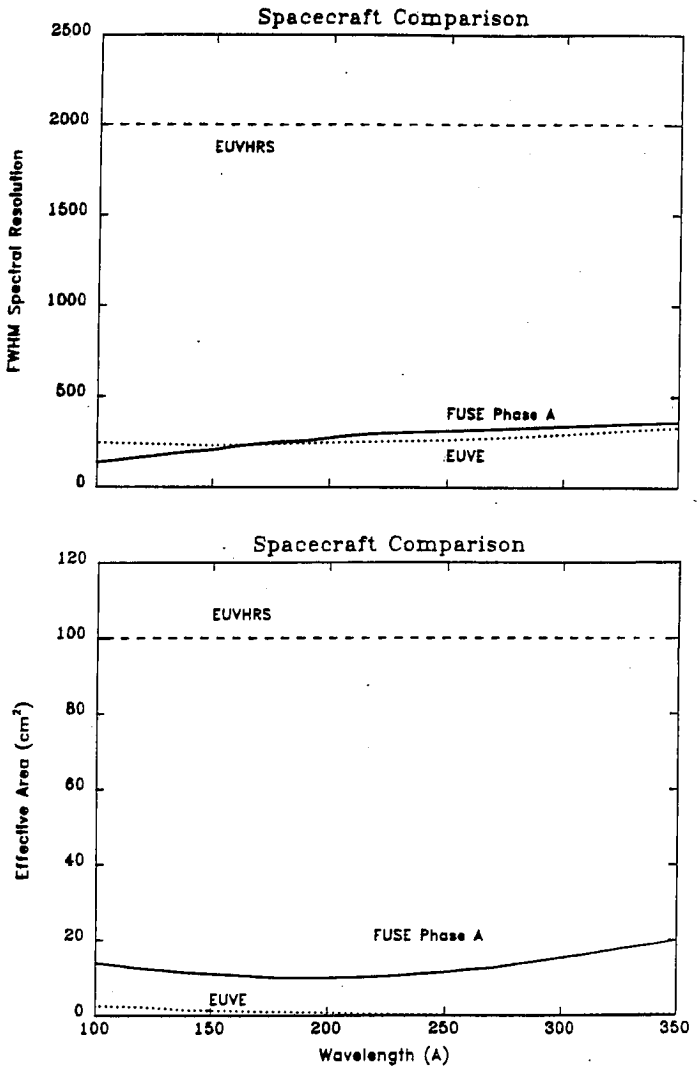

Figure 2: Comparison of different EUV spectrometers. (top) Spectral resolution of the spectrometer on the EUVE satellite, the high-throughput channel of the spectrometer described in the Lyman/FUSE Phase A Report /10/, and a hypothetical high-resolution spectrometer (EUVHRS). (bottom) Effective areas for these three spectrometers.

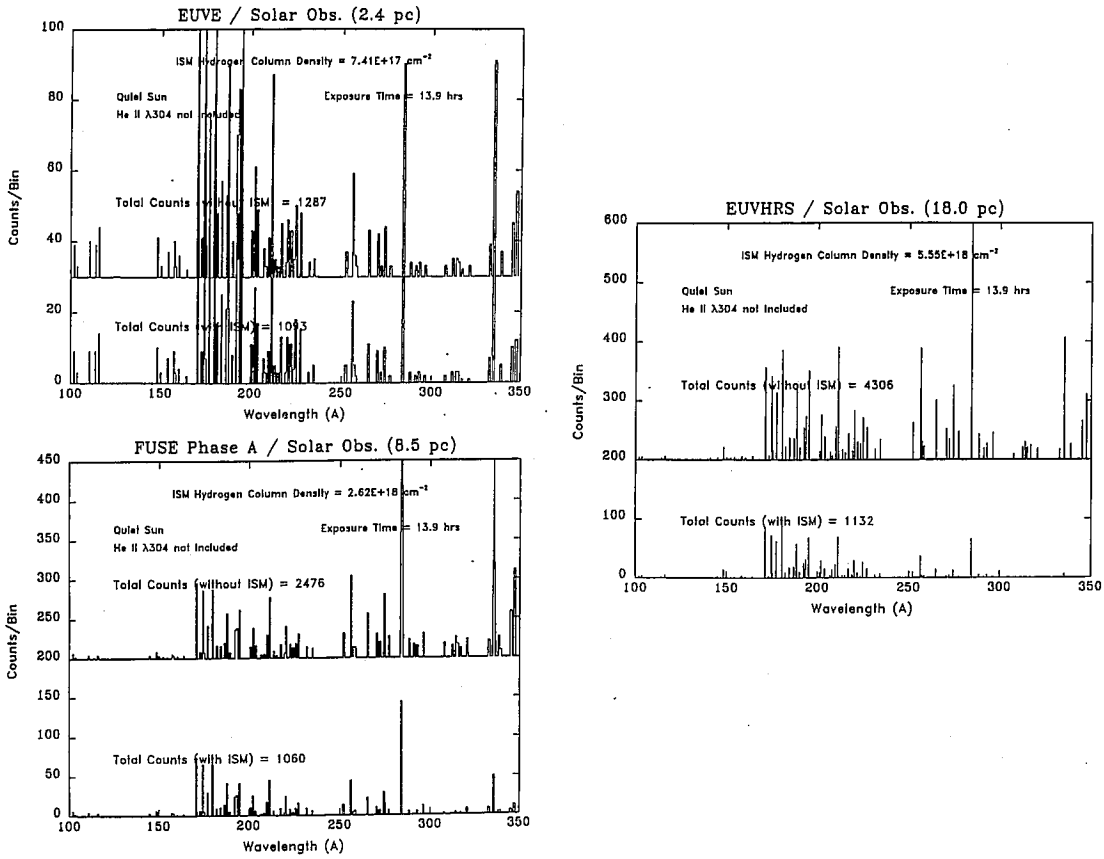

Figure 3: Comparison of predicted spectra for the average quiet Sun as folded through the response functions of the three spectrometers described in Fig. 2. Each panel consists of the intrinsic spectrum (ignoring the HeII 304 Å line) displaced upwards, and the spectrum including interstellar absorption with the indicated neutral hydrogen column density computed for $n_H = 0.1$ cm^{-3} and the indicated distance such that the total counts including interstellar absorption exceed 1000 in 50,000 seconds. (top) Calculated spectra in counts per spectral bin for the EUVE spectrometer. (bottom) Same for the Lyman/FUSE Phase A spectrometer. (right) Same for the EUVHRS spectrometer.

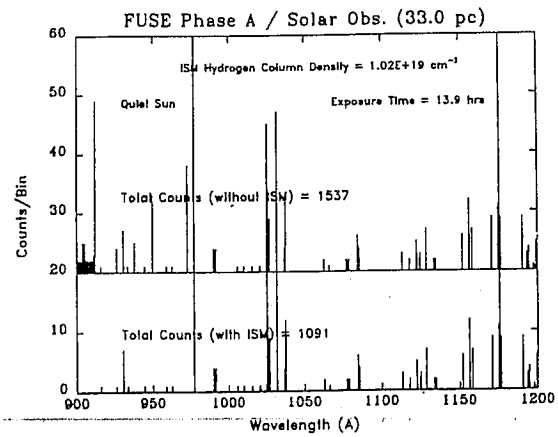

Figure 4: Comparison of predicted spectra in the 900–1200 Å region for the quiet Sun as folded through the Lyman/FUSE prime spectrometer parameters /10/. Plotted are the intrinsic spectrum (displaced upwards) and the spectrum including absorption by interstellar hydrogen (continuum and lines) for the indicated distance and $n_H = 0.1$ cm^{-3}. The source distance was obtained by requiring that the total counts exceed 1000 in 50,000 seconds including interstellar absorption.

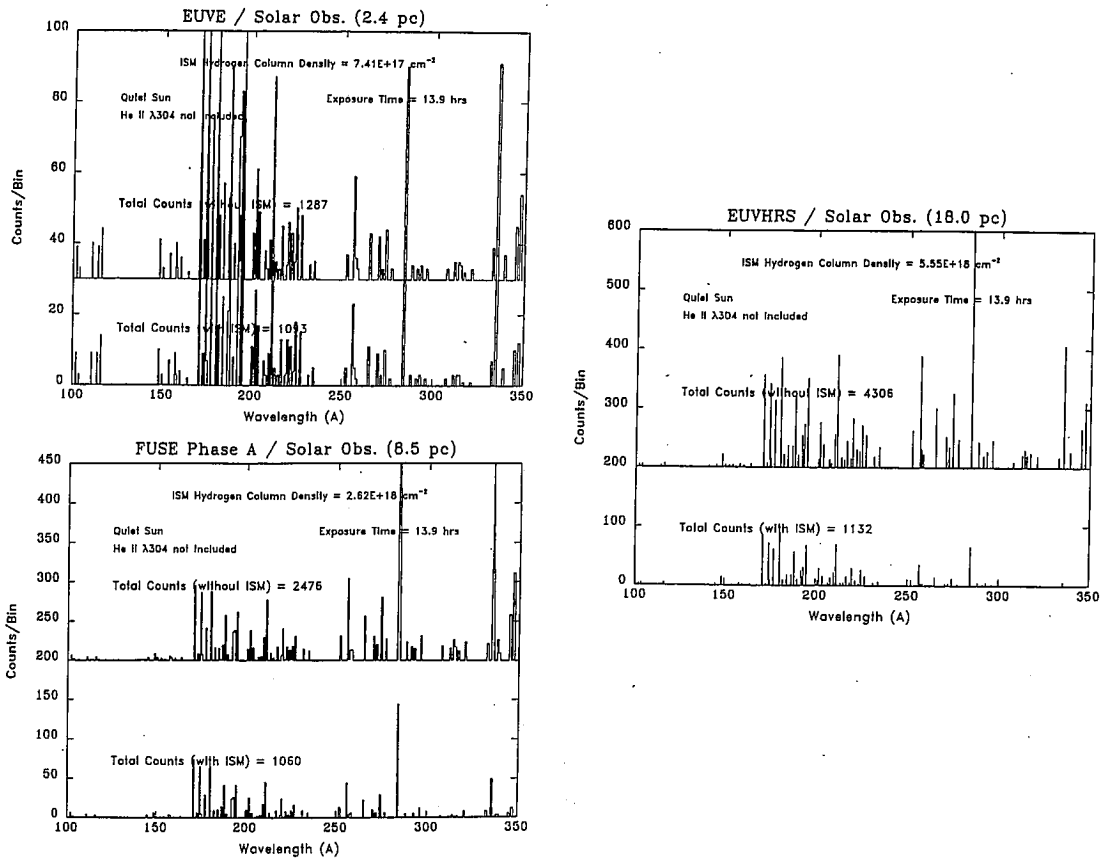

Figure 3: Comparison of predicted spectra for the average quiet Sun as folded through the response functions of the three spectrometers described in Fig. 2. Each panel consists of the intrinsic spectrum (ignoring the HeII 304 Å line) displaced upwards, and the spectrum including interstellar absorption with the indicated neutral hydrogen column density computed for $n_H = 0.1$ cm^{-3} and the indicated distance such that the total counts including interstellar absorption exceed 1000 in 50,000 seconds. (top) Calculated spectra in counts per spectral bin for the EUVE spectrometer. (bottom) Same for the Lyman/FUSE Phase A spectrometer. (right) Same for the EUVHRS spectrometer.

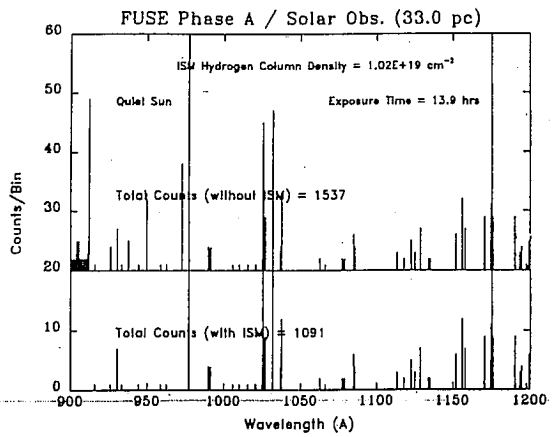

Figure 4: Comparison of predicted spectra in the 900–1200 Å region for the quiet Sun as folded through the Lyman/FUSE prime spectrometer parameters /10/. Plotted are the intrinsic spectrum (displaced upwards) and the spectrum including absorption by interstellar hydrogen (continuum and lines) for the indicated distance and $n_H = 0.1$ cm^{-3}. The source distance was obtained by requiring that the total counts exceed 1000 in 50,000 seconds including interstellar absorption.

The intrinsic spectrum of the RS CVn-type system AR Lac was computed using the two-temperature emission measure distribution derived from *Einstein* Solid State Spectrometer data /11/. The photon flux near 100 Å, which is comparable to that in the soft x-ray region and contains information on the coronal emission measure over a similar range of temperatures. The predicted spectra of AR Lac for 50,000 seconds exposure are shown in Figure 5(left) both before and including interstellar absorption for the three spectrometers. In each case a high signal/noise EUV spectrum can be obtained in far less that 50,000 seconds.

The importance of high throughput is illustrated in Figure 5(right), where we compute spectra for σ CrB during its flare on 1983 September 29 /12/. For each spectrometer the exposure time was taken to be 1 minute at the flare peak emission measure to study the time development of the flaring plasma. In this simulation the EUVE spectrometer provides very few photons (although an acceptable number in a 10 minute integration), while the other two spectrometers provide good statistics in only 1 minute integrations.

The importance of simultaneous high spectral resolution and high throughput is illustrated in Figure 6, which shows simulated spectra of the FeXX 133 Å line from AR Lac folded through the EUVHRS. For this simulation half of the stellar flux is assumed to be uniformly distributed across the surface of the K0 IV star and the other half within a small coronal structure located at different projected radial distances from the center of the star and co-rotating with the star whose surface equatorial rotational velocity is 70 km s^{-1}. The influence of the active region on the detected line profile indicates that the EUVHRS can locate bright regions in the corona of this star using the Doppler imaging technique /13/.

In our final simulation (Figure 7) we show that the Prime spectrometer of Lyman/FUSE has sufficient spectral resolution and effective area to measure Doppler shifts in the transition region of a star similiar to a solar active region but located at the distance of the Hyades. The counting statistics are sufficient to measure a Doppler shift as small as 2-3 km s^{-1} due either to a stellar wind (blue shift) or to downflows in magnetic flux tubes /14/.

HOW MANY STARS MAY BE DETECTED IN THE EUV?

The Wide Field Camera on ROSAT will soon tell us how many stars of different spectral types are detectable with broad-band photometry in the EUV. Prior to the start of their survey, we would like to hazard some guesses concerning how many may be detected spectroscopically in the off chance that we may be right. Table 2 lists the number densities of RS CVn, W UMa, and dMe stars estimated from the *Einstein* Medium Sensitivity Survey (EMSS) /15/ and an estimate for the cataclysmic variables /16/. Using these space densities, we list in Table 3 the number of objects out to a range of distances that lie within a hydrogen column density of $N_H \leq 10^{19}$ cm^{-2} estimated using the LISM map of Paresce /9/. This value of N_H corresponds to 20% transmission at 200 Å and 80% transmission at 100 Å. The detection horizons for the three spectrometers summarized in Table 4 indicate that each instrument could detect many of each class of object.

Table 2. Number Densities of Different Types of Stars

Star Type	Density (pc^{-3})	Reference
RS CVn	$2.89 \pm 0.62 \times 10^{-4}$	EMSS /15/
W UMa	$6.55 \pm 2.07 \times 10^{-5}$	EMSS /15/
dMe	$2.40 \pm 0.38 \times 10^{-2}$	EMSS, $\log(L_x) \geq 27.8$
CV	6×10^{-6}	Patterson /16/

Table 3. Number of Stars within d(pc) for $N_H \leq 10^{19}$ cm^{-2}

d(pc)	N(RS CVn)	N(W UMa)	N(dMe)	N(CV)
10	0.6	0.14	50	0.01
20	4	1	300	0.1
30	12	3	900	0.3
50	20	6	1600	0.6
100	340	100	30,000	8
200	1600	500	150,000	40

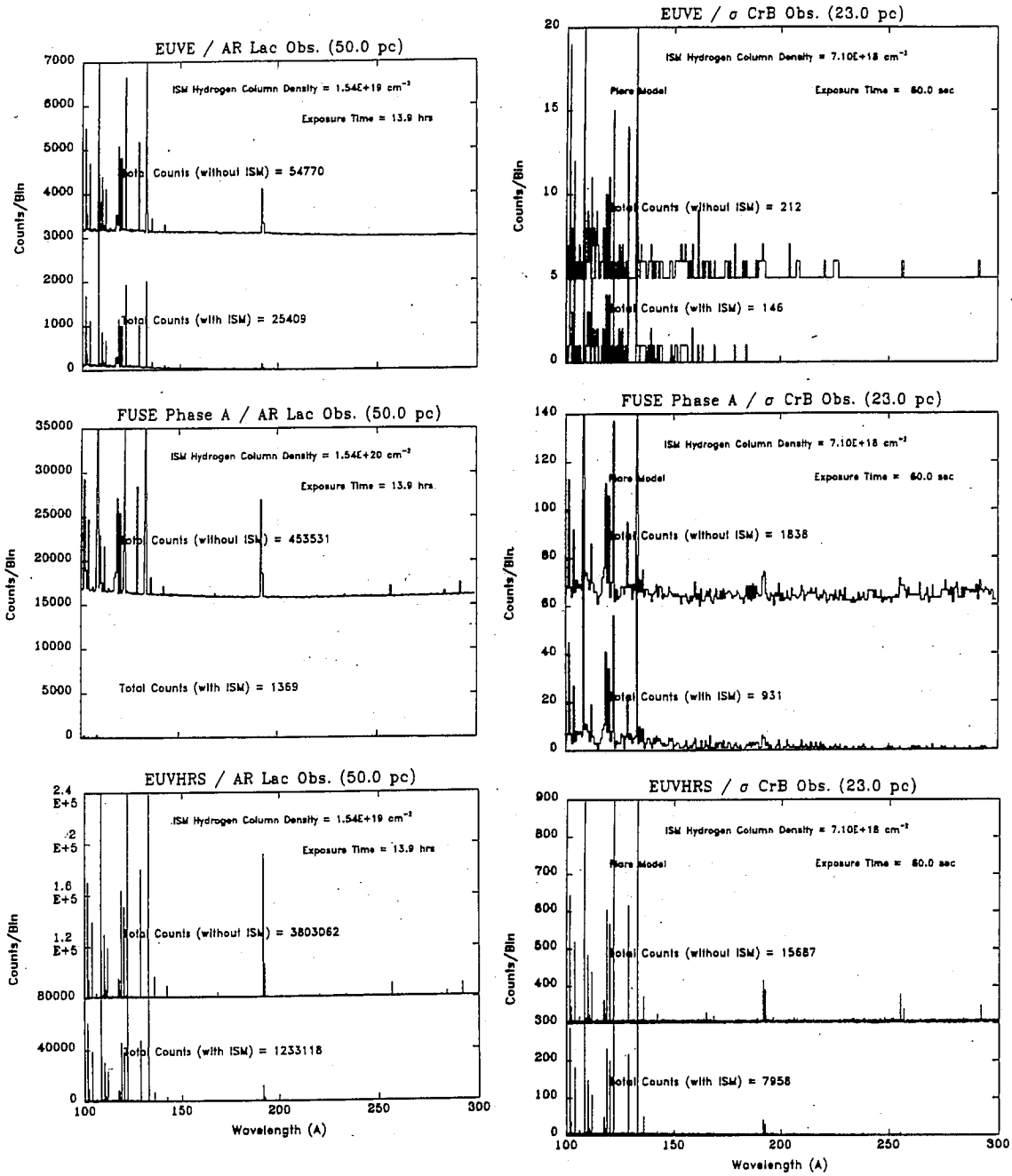

Figure 5: (left panels) Comparison of predicted spectra of AR Lac for 50,000 seconds exposure. Each panel consists of the computed spectrum without interstellar absorption (displaced upwards) and including interstellar absorption with the indicated hydrogen column density – (top) for the EUVE spectrometer, (middle) for the Lyman/FUSE Phase A spectrometer in its high-throughput mode, (bottom) for the EUVHRS spectrometer. (right panels) Predicted spectra from σ CrB for a 1 minute integration assuming the peak emission measure (5.7×10^{53} cm^{-3}) and temperature (9.5×10^{7} K) for the 29 September 1983 flare observed by EXOSAT /12/ – (top) for the EUVE spectrometer, (middle) for the Lyman/FUSE Phase A spectrometer in its high-throughput mode, (bottom) for the EUVHRS spectrometer.

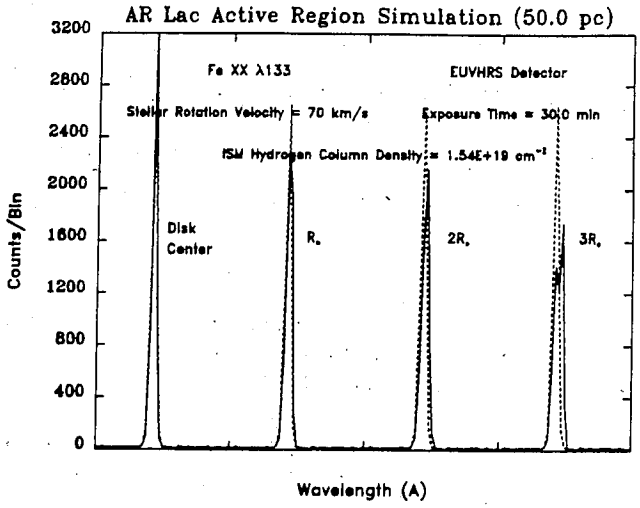

Figure 6: Simulated spectra of the FeXX 133 Å line from AR Lac as observed by the EUVHRS spectrometer with a 30 minute integration including interstellar absorption. Half of the flux is assumed to be uniformly distributed across the stellar surface and the other half concentrated in a small active region that corotates with the star (equatorial rotational velocity of 70 km s^{-1}). For each simulation the dashed line is a comparison profile in which all of the flux is uniformly distributed across the stellar surface. The active region is placed at disk center (left), at the limb (second from left), and at 1 and 2 stellar radii above the limb.

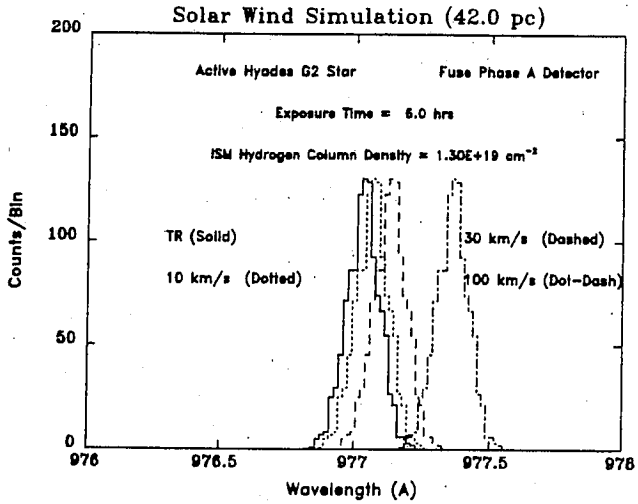

Figure 7: Simulated spectra of the CIII 977 Å line observed by the Lyman/FUSE Prime Spectrometer from an active G2V star located in the Hyades cluster. The simulated spectra are for the line formed in a region at rest and with Doppler shifts of 10, 30, and 100 km s^{-1}. The vertical scale is counts per spectral bin assuming a resolution of 30,000.

Table 4. Detection Horizon (pc)

Spectrometer	Detection Criterion 10^3 counts in 10^5 seconds				
	Quiet Sun	Active Sun	dMe	AR Lac	AS(FUV)
EUVE	2.4	6.5	10	250	–
FUSE Phase A	8.5	19	30	600	100
EUVHRS	18	36	60	2000	–

CONCLUSIONS

We conclude that while each of the spectrometers will detect a number of stellar sources, high throughput and spectral resolution are needed for such detailed physical studies as Doppler imaging, measurements of stellar winds and downflows, and high time resolution studies of stellar flares.

We wish to thank Dr. Alex Brown for providing us with the plasma spectroscopy code, Dr. Webster Cash and Mr. Erik Wilkinson for providing an early version of the code for simulating the instrumental response function, Dr. Tom Fleming for providing space density estimates for different types of stars prior to publication, and Dr. M. Shull for comments on the text. This work is supported by interagency transfer H-80531-B from NASA to the NIST and NASA grant NAG5-82 to the University of Colorado.

REFERENCES

1. A.K. Dupree, M.C.E. Huber, R.W. Noyes, W.H. Parkinson, E.M. Reeves, G.L. Withbroe, The extreme-ultraviolet spectrum of a solar active region, *Ap. J.* **182**, 321 (1973).

2. J.L. Linsky, P.L. Bornmann, K.G. Carpenter, R.F. Wing, M.S. Giampapa, S.P. Worden, and E.K. Hege, Outer atmospheres of cool stars. XII. A survey of IUE Ultraviolet emission line spectra of cool dwarf stars, *Ap. J.* **260**, 670 (1982).

3. P.B. Byrne, J.G. Doyle, A. Brown, J.L. Linsky, and M. Rodonò, Rotational modulation and flares on RS CVn and BY Dra stars. VI. Physical parameters of the chromospheres/transition regions of V 711 Tau (HR 1099), H Peg and AR Lac during October 1981, *Astr. Ap.* **180**, 172 (1987).

4. R.D. Chapman and W.M. Neupert, Slowly varying component of extreme ultraviolet solar radiation and its relation to solar radio radiation, *J. Geophys. Res.* **79**, 4138 (1974).

5. S.O. Kastner, W.M. Neupert, and M. Swartz, Solar-flare emission lines in the range from 66 to 171 Å; $2s^r2p^k - 2s^{r-1}2p^{k+1}$ transitions in highly ionized iron, *Ap. J.* **191**, 261 (1974); C. Jordan, The Ionization Equilibrium of Elements Between Carbon and Nickel, *M.N.R.A.S.* **142**, 501 (1969).

6. K.P. Dere, H.E. Mason, K.G. Widing, and A.K. Bhatia, XUV electron density diagnostics for solar flares, *Ap. J. Suppl.* **40**, 341 (1979).

7. U. Feldman, The use of spectral emission lines in the diagnostics of hot solar plasmas, *Physics Scripta* **24**, 681 (1981).

8. P.C. Frisch and D.G. York, Synthesis maps of ultraviolet observations of neutral hydrogen gas, *Ap. J. (Letters)* **271**, L59 (1983).

9. F. Paresce, On the distribution of interstellar matter around the Sun, *A. J.* **89**, 1022 (1984).

10. LYMAN: The Far Ultraviolet Spectroscopic Explorer, Phase A Study Final Report, July 1989.

11. J.H. Swank, N.E. White, S.S. Holt, and R.H. Becker, Two-component x-ray emission from RS CVn binaries, *Ap. J.* **246**, 208 (1981).

12. G.H.J. van den Oord, R. Mewe, and A.C. Brinkman, An EXOSAT Observation of an X-ray Flare and Quiescent Emission from the RS CVn Binary σ CrB, *Astr. Ap.* **205**, 181 (1988).

13. J.E. Neff, F.M. Walter, M. Rodonò, and J.L. Linsky, Rotational Modulation and Flares on RS CVn and BY Dra Stars. XI. Ultraviolet Spectral Images of AR Lac in September 1985, *Astr. Ap.* **215**, 79 (1989).

14. T.R. Ayres, E. Jensen, and O. Engvold, Redshifts of High-temperature Emission Lines in the Far-Ultraviolet Spectra of Late-type Stars. II. New, Precise Measurements of Dwarfs and Giants, *Ap. J. Suppl.* 66, 51 (1988).

15. T.A. Fleming, private communication. For previous estimates see *A. J.* **98**, 692 (1989) and *Ap. J.* **331**, 958 (1988).

16. J. Patterson, The Evolution of Cataclysmic and Low-mass X-ray Binaries, *Ap. J. Suppl.* **54**, 443 (1984).